

AN INVESTIGATION OF MASS COMPOSITION OF ULTRA-HIGH ENERGY COSMIC RAYS WITH ENERGIES ABOVE 10^{19} eV VIA THE STUDY OF EXTENSIVE AIR SHOWERS

S. Doostmohammadi and S. J. Fatemi

Faculty of Physics, Shahid Bahonar University of Kerman, Kerman 76169-14111, Iran

E-mail: doostmohammadi@sci.uk.ac.ir

(Received: January 7, 2012; Accepted: February 20, 2012)

SUMMARY: The electron and muon components of extensive air shower (EAS) with energies above 10^{19} eV are analyzed via various giant EAS arrays. A varying property of showers is observed for two energy ranges; higher and lower than $(3 - 4) \times 10^{19}$ eV. The age parameter, zenith angle, shower size dependence on muon size and shower size dependence on primary energy show an increment of mass composition (MC) above $(3 - 4) \times 10^{19}$ eV. Comparison of the observed EAS results with the simulations of Capdevielle et al. (2000) and Shinozaki et al. (2005) gives at most 20% photon fraction for primary energies above 10^{19} eV. The arrival directions of showers above 4×10^{19} eV indicate an increasing concentration towards the super galactic plane.

Key words. cosmic rays

1. INTRODUCTION

The composition of ultra-high energy cosmic rays (UHECRs), especially above 4×10^{19} eV, is still unknown. Determination of the type of the primary cosmic ray (CR) particles is a clue for understanding the origin and mechanism(s) of their production. The distance of the source relative to the Earth cannot be much more than a few tens of Mpc due to GZK cut off (Greisen 1966) (i.e. the energy loss of particles during their travel and interaction with universal background radiation). Owing to the observation of CRs with energies exceeding GZK cut off ($E_{GZK} \sim 4 \times 10^{19}$ eV), it is proposed that the CRs excess can be due to two astrophysical origins based on two different approaches. One is the top-down scenario which is a no-acceleration approach (i.e. decay of certain sufficiently massive particles), and the

other is the bottom-up scenario which is the more conventional acceleration approach (i.e. acceleration due to diffusive shock processes). The two scenarios predict different photon fractions in UHECR and we simulated this fraction via the two corresponding models. Qualitatively, the fraction prediction of primary photons varies from 10% to 50% for the top-down model and is about 0.1% for the bottom-up model. (For more details on the models and their expected primary photons see Bhattacharjee and Sigl 2000). There are contradictory results on primary photon fractions and their astrophysical origins at highest energies from an experimental point of view. For example, the AGASA group claimed high fraction of primary photons supporting the top-down scenario (Risse et al. 2005) but the Auger observatory group disagrees with this claim. (Healy 2007). Revealing the true composition of the primary CR

spectrum, and especially its photon fraction, is essential for distinguishing between the two models. Investigation of the muon component of EAS, which is a sensitive and main parameter of the mass composition (MC) of EAS, is also desired to study the above subject. In this paper, the high quality data of Yakutsk (Efimov et al. 1988), Haverah Park (University of Leeds 1980) and Volcano Ranch (University of New Mexico 1980) EAS arrays are used. The zenith angle distribution, age parameter and also $N_e - E_p$ relation are used as important parameters to determine MC of CRs at highest energies.

2. OBSERVABLES FOR MASS DISCRIMINATION

2.1. The age parameter

Our intention is to explore the EAS properties which bear information of MC in the primary energy range (i.e. above 10^{19} eV). In this paper, the universal data including the EAS array data of Yakutsk (at sea level) and Volcano Ranch (at height 1700 meters relative to the sea level) are used. These data consist of a set of electron densities, Δ_e , their core distance r , the primary energy E_p , and zenith angle θ , for each array. The age parameter is the first quantity considered to be sensitive to the primary MC. It is described by electromagnetic cascade theory (Nishimura 1958) as the stage of shower development in the atmosphere whose value increases with its development. This theory predicts that the shower age would decrease with increasing energy E , but if the MC of particles initiating the shower changes (e.g. proton to iron), the age parameter would increase with increasing energy.

The increment of age parameter with MC has been pointed out already by other researchers. For example, its increment was specified by Ivanov et al. (2011). We have also demonstrated this increment by calculating the variation of β (Delta Beta) and then by its drawing as a function of shower age s by using the data from Ivanov et al. (2011), which are deduced from Fig. 1 (β is the slope parameter of lateral distribution function (LDF) of electrons) Since iron has a wider LDF of electrons than proton, so it relatively has a longer age.

The LDF of electrons of Nishimura-Kamata-Greisen (NKG) is used to determine the age of each shower as follows:

$$\rho_e(r) = \frac{N_e}{r_0^2} F\left(\frac{r}{r_0}\right) \quad (1)$$

where $\rho_e(r)$ is the electron density at the core distance r (in r_0 unit), N_e is the shower size, and:

$$F\left(\frac{r}{r_0}\right) = c(s) \left(\frac{r}{r_0}\right)^{s-2} \left(1 + \frac{r}{r_0}\right)^{s-4.5} \quad (2)$$

where s is the shower age, $c(s)$ is a function of s , and r_0 is the Moliere unit.

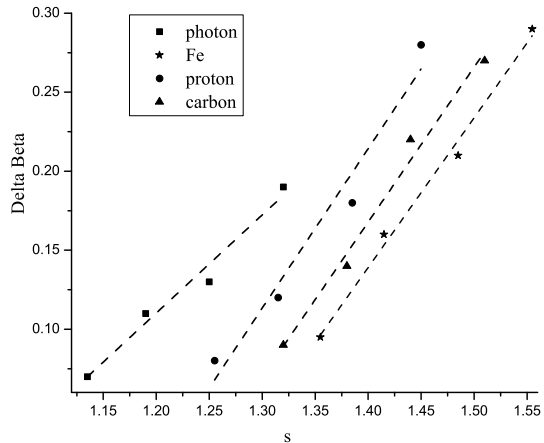


Fig. 1. The slope variation of LDF of electrons as a function of age parameter for different mass composition calculated from the data of Ivanov et al. (2011).

The given parameters of EAS data which are used in Eq. (1) are electron densities, core distance and Moliere unit. Eq. (1) is then minimized to obtain N_e and s . This is done for every shower data of the two arrays. Fig. 2 shows the dependence of age parameter on the primary energy. A change towards increase of the age parameter at $(3-4) \times 10^{19}$ eV reflects an increment of MC above this energy. The results of the two arrays, Volcano Ranch Fig. 2a at high altitude and Yakutsk Fig. 2b at sea level, show the same increasing effect which is consistent with the results of Mikhailov et al. (2005)

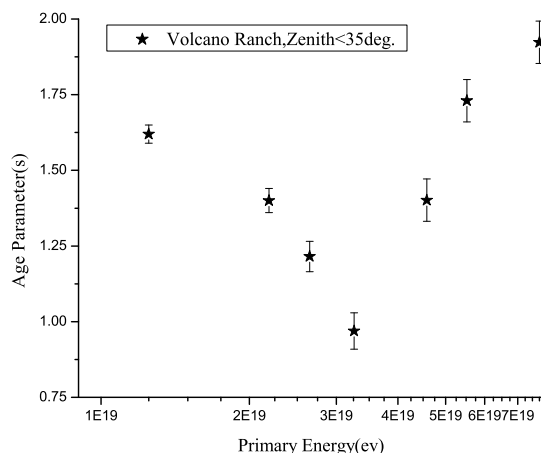


Fig. 2a. The dependence of age parameter on primary energy with zenith angle less than 35° for Volcano Ranch at 1700 meter altitude. The increase of average age is observed at $E > 4 \times 10^{19}$ eV.

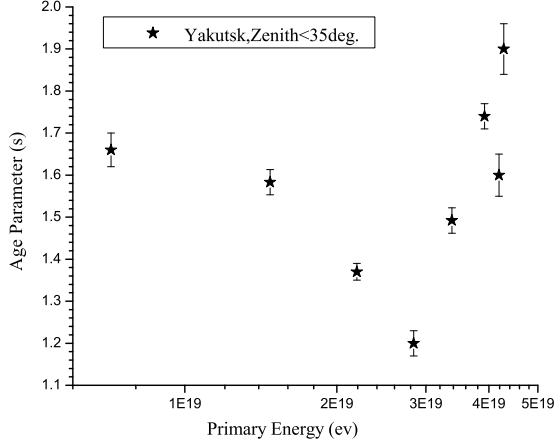


Fig. 2b. The dependence of age parameter on primary energy with zenith angle less than 35° for Yakutsk array at about sea level. The increase of average age is observed at $E > 4 \times 10^{19}$ eV.

2.2. The relation between the shower size (N_e) and the primary energy (E_p)

Here, we obtain the dependence of N_e on E_p based on zenith angle for two ranges: lower and higher than 35° . In both ranges there is a change in the vicinity of 4×10^{19} eV, what confirms the shower age or MC change at this energy. The shower size at a fixed E_p for $\theta > 35^\circ$ is smaller than that for $\theta < 35^\circ$, which is due to a longer path and more attenuation in the atmosphere. Variation of MC to

heavier masses (e.g. proton to iron) results in a much smaller energy contribution for every proton produced by primary heavy masses. So, these protons develop lower in the atmosphere and get more attenuated. Therefore, a lower N_e is detected for 4×10^{19} eV at detector array level (as shown in Fig. 3) with much sharper increase of N_e in terms of energy (as shown in Fig. 3, Table (1a) and Table (1b)). These results are calculated for Haverah Park and Yakutsk arrays at about the sea level, and also for Volcano Ranch array at 1700 m altitude. The results from all three arrays show the same effect on N_e indicating the change of MC above energies higher than 4×10^{19} eV which are all given in the Tables (1a) and (1b).

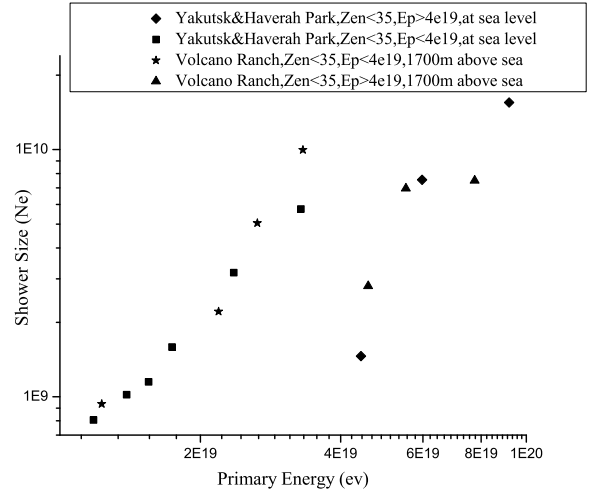


Fig. 3. The $N_e - E_p$ dependence. N_e has a sharp drop and a faster increase at 4×10^{19} eV.

Table 1a. $N_e - E_p$ correlation. Haverah Park and Yakutsk arrays, at about sea level.

	$E_p < 4 \times 10^{19}$ eV	$E_p > 4 \times 10^{19}$ eV
$\theta < 35^\circ$	$N_e = A_1 \exp\left(\frac{-E_p}{t_1}\right) + A_2 \exp\left(\frac{-E_p}{t_2}\right) + (9.2 \times 10^8)$ $A_1 = 2E7, t_1 = -6.1E18,$ $A_2 = 2E7, t_2 = -6.1E18$	$N_e = A_1 \exp\left(\frac{-E_p}{t_1}\right) + A_2 \exp\left(\frac{-E_p}{t_2}\right) + (7.6 \times 10^9)$ $A_1 = -1E13, t_1 = 5.4E18,$ $A_2 = -1E13, t_2 = 5.4E18$
$\theta > 35^\circ$	$N_e = A_1 \exp\left(\frac{-E_p}{t_1}\right) + A_2 \exp\left(\frac{-E_p}{t_2}\right) + (4 \times 10^8)$ $A_1 = 2.2E7, t_1 = -9.6E18,$ $A_2 = 2.2E7, t_2 = -9.6E18$	$N_e = A_1 \exp\left(\frac{-E_p}{t_1}\right) + A_2 \exp\left(\frac{-E_p}{t_2}\right) + (2.8 \times 10^{10})$ $A_1 = -3.02E11, t_1 = 1.62E19,$ $A_2 = -2.84E11, t_2 = 1.64E19$

Table 1b. $N_e - E_p$ correlation. Volcano Ranch arrays at about 1700 m altitude.

	$E_p < 4 \times 10^{19} \text{eV}$	$E_p > 4 \times 10^{19} \text{eV}$
$Zen < 35^\circ$	$N_e = A_1 \exp\left(\frac{-E_p}{t_1}\right) + A_2 \exp\left(\frac{-E_p}{t_2}\right) + (4 \times 10^8)$ $A_1 = 2.2E7, t_1 = -9.6E18,$ $A_2 = 2.2E7, t_2 = -9.6E18$	$N_e = A_1 \exp\left(\frac{-E_p}{t_1}\right) + A_2 \exp\left(\frac{-E_p}{t_2}\right) + (1 \times 10^{10})$ $A_1 = -2.3E12, t_1 = 6.7E18,$ $A_2 = -2.3E12, t_2 = 6.7E18$
$Zen > 35^\circ$	$N_e = A_1 \exp\left(\frac{-E_p}{t_1}\right) + A_2 \exp\left(\frac{-E_p}{t_2}\right) + (4.4 \times 10^7)$ $A_1 = 3.2E7, t_1 = -1.1E19,$ $A_2 = 3.2E7, t_2 = -1.1E19$	$N_e = A_1 \exp\left(\frac{-E_p}{t_1}\right) + A_2 \exp\left(\frac{-E_p}{t_2}\right) + (3.3 \times 10^8)$ $A_1 = 51.2, t_1 = -3.6E18,$ $A_2 = 51.2, t_2 = -3.6E18$

2.3. Zenith angle distribution

The zenith angle distribution (ZAD) is indirectly another sensitive parameter for studying MC. The results of ZAD versus energy are shown in Fig. 4 indicating that ZAD is different for showers of two energy ranges: lower and higher than about $4 \times 10^{19} \text{eV}$. The arrival direction differences were also shown in the latitude distribution of galactic and super galactic planes in the paper of Kermani and Fatemi (2011) in which there is a consistency between the arrival direction of Auger EAS events of energy above 50 EeV (exa electron volts) and super galactic plane which is not observed in the lower energy range (lower than 40 EeV), indicating different sources and MCs for lower and higher energies than $4 \times 10^{19} \text{eV}$.

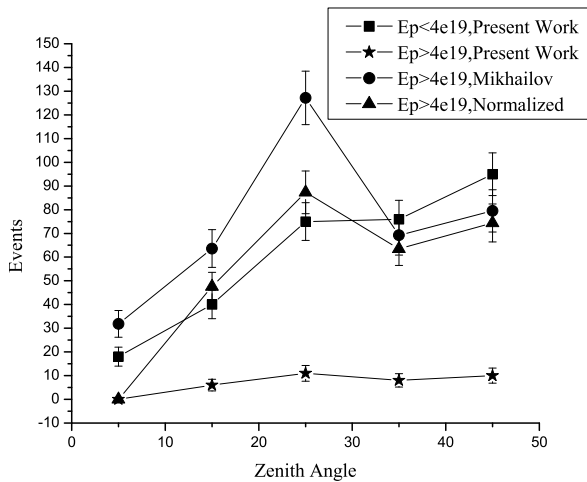


Fig. 4. The zenith angle distributions for energies smaller and greater than 40EeV . The distribution peaks for higher energies what is not observed for smaller energies. The result of Mikhailov et al. (2005) is also shown for comparison.

2.4. Muon size

The muon size of a shower is a qualitative and sensitive parameter to study MC of very high energy CRs. The results of two muon simulations are investigated: one is the simulation of Capdevielle et al. (2000) and the other is the simulation of Shinozaki et al. (2005) which are used for primary Gamma, proton and iron particles by using $\rho_\mu(1000)$ (i.e. the muon density at distance of 1000 meters from the core). To compare the muon array data with the muon simulations of Capdevielle et al. (2000), the muon size N_μ of array data has to be calculated by using the two muon formulas as follows:

(i) Hayashida et al. (1995) equation:

$$\rho_\mu(r) = N_\mu \left(\frac{c_\mu}{R_0^2}\right) r^{-\alpha} (1+r)^{-\beta} \left[1 + \left(\frac{R}{800}\right)^3\right]^{-\delta}, \quad (3)$$

where $r = \frac{R}{R_0}$, R is core distance, and:

$c_\mu = 0.262$ for $R < 800$ meters,

$c_\mu = 0.325$ for $R > 800$ meters,

$\beta = 2.52$, $\delta = 0.6$, $\alpha = 0.75$,

$R_0 = 0.66$ for $\text{sect}\theta < 1.1$,

$\text{Log}R_0 = 0.58(\text{sect}\theta - 1) + 2.39$ for $1.1 < \text{sect}\theta < 1.8$.

(ii) Luczak et al. (2009) equation:

$$\rho_\mu(r) = \frac{0.28N_\mu}{r_0^2} \left(\frac{r}{r_0}\right)^{p_1} \left(1 + \frac{r}{r_0}\right)^{p_2} \left[1 + \left(\frac{r}{10r_0}\right)^2\right]^{p_3} \quad (4)$$

where r is core distance, $p_1 = -0.69$, $p_2 = -2.93$, $p_3 = -1$ and $r_0 = 320$ m. Both results are shown in Fig. 5 which reflects a mixed Gamma-proton and Gamma-heavy nucleus. This is consistent with the previous works of Auger group (Healy 2007) (which gives domination of iron at a few 10^{19}eV) and Mikhailov et al. (2005) (with their results showing

a heavier MC than iron for $E_p > 4 \times 10^{19}$ eV). Also, they observe a few percent of primary photons what does not favor the predictions of top-down models but is consistent with the previous work of the Auger observatory group at energies above 10^{19} eV (Healy 2007, Risse and Homala 2007)

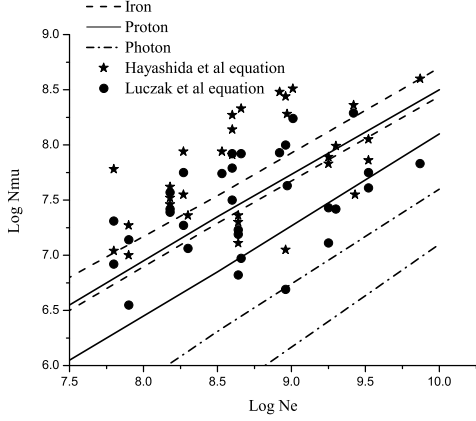


Fig. 5. Scatter plot of muon-electron sizes, calculated from muon LDF formula in comparison with simulation work of Capdevielle et al. (2000) A very heavy component of a mixed MC is seen at the highest energy.

Also, to use the simulation of Shinozaki et al. (2005) the muon densities at core distance of 1000 m (i.e. $\rho_\mu(1000)$) are needed. These are calculated from the measured muon density of Yakutsk array at distance r via converting it to 1000 m by using the Supanitsky et al. (2005) equation:

$$\rho_\mu(r) = p_0 \left(\frac{r}{r_0}\right)^{-\alpha} \left(1 + \frac{r}{r_0}\right)^{-\beta} \left[1 + \left(\frac{r}{10r_0}\right)^2\right]^{-\gamma}, \quad (5)$$

where r is core distance, $\alpha = 0.75$, $\gamma = 2.93$, and $r_0 = 320$ m. p_0 and β are free fit parameters.

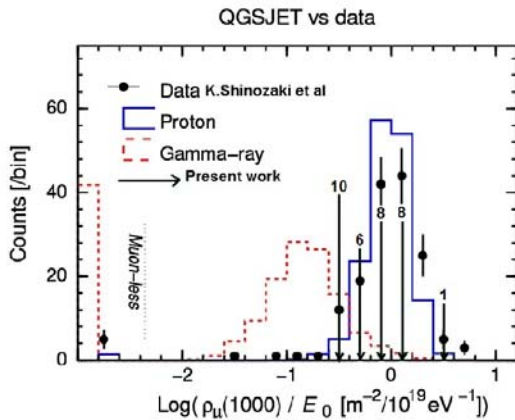


Fig. 6. Comparison of the fraction of muon density $\frac{\rho_\mu(1000)}{(E_p) \times 10^{-19}}$, calculated using Eq. (5), with the simulated one. (Shinozaki et al. 2005).

The comparison of the calculated fraction with the corresponding simulated fraction of $\frac{\rho_\mu(1000)}{(E_p) \times 10^{-19}}$ is shown in Fig. 6 which indicates an upper limit of 20% on primary photons.

CONCLUSION

It is shown that the parameters which are sensitive to the mass composition of UHECR (the age parameters, the muon size, and indirectly the zenith angle distribution) differ for primary energies below and over 4×10^{19} eV, leading to the conclusion that the primaries with energies higher than this value are of a much heavier composition. The comparison of the observed and simulated fractions of primary photons leads to an upper limit of about 20% for the photon fraction what suggests the absence of photon candidates for events above 10EeV. The results do not support the top-down, non-accelerator model. Arrival directions of primaries with energies above $(4 - 5) \times 10^{19}$ eV concentrate on the super galactic plane.

Acknowledgements – We are grateful to the high energy astrophysics group of Adelaide University. We also thank prof. R. Clay on sabbatical leave to Australia in 2007-2008 for his great scientific support and for providing the EAS array data used in this work.

REFERENCES

- Bhattacharjee, P., Sigl, G.: 2000, *Phys. Rep.*, **327**, 109.
- Capdevielle, J. N., Le Gall C., Sanosyan, N.: 2000, *Astropart. Phys.*, **13**, 259.
- Efimov, N. N., Egorov, T. A., Krasilnikov, D. D., Pravdin, M. I., Sleptsov, I. Ye.: 1988, *world data center of Yakutsk arrays*.
- Greisen, K.: 1966, *Phys. Rev. Lett.*, **16**, 748.
- Hayashida, N., Honda, K., Honda, M., Imaizumi, S.: 1995, *J. Phys. G. Nucl. Partic.*, **21**, 1101.
- Healy, M. D.: 2007, *20th ICRC Mexico*, **4**, 377.
- Ivanov, A. A., Pravdin, M. I., Sabourov, A. V.: 2011, *32nd ICRC, Beijing*.
- Kermani, H. A., Fatemi, S. J.: 2011, *Iran. J. Phys. Res.*, **10**, No 4.
- Luczak, P., Apel, W. D., Arteaga, J. C., Badea, F., Bekk, K.: 2009, *Proceedings of The 31st ICRC, LODZ*.
- Mikhailov, A. A., Efremov, N. N., Gerasimova, N. S., Makarov, I. T.: 2005, *29th ICRC Pune*, **7**, 227.
- Nishimura: 1958, *Prog. Theor. Phys. Supp*, **6**, 93.
- Risse, M., Homala, P., Engel, R., Gora, D.: 2005, *Phys. Rev. Lett.*, **95**, 171102.
- Risse, M., Homala, P.: 2007, *Mod. Phys. Lett. A*, **22**, 749.
- Shinozaki, K., Chikawa, M., Fukushima, M., Hayashida, N.: 2005, *29th ICRC Pune*, **7**, 151.
- Supanitsky, D., Tiba, A., Medina-Tanco, G., Etchegoyen, I.: 2005, *29th ICRC Pune*, **7**, 37.

World Data center for cosmic rays, Catalogue of highest energy cosmic rays, 1980. University of new mexico, (Volcano Ranch Arrays).

World Data center for cosmic rays, Catalogue of highest energy cosmic rays, 1980. University of Leeds, (Haverah Park Arrays).

О МАСЕНОМ САСТАВУ ПРИМАРНОГ КОСМИЧКОГ ЗРАЧЕЊА СА ЕНЕРГИЈАМА ВЕЋИМ ОД 10^{19} eV НА ОСНОВУ ПРОУЧАВАЊА ШИРОКИХ АТМОСФЕРСКИХ ЛАВИНА КОСМИЧКОГ ЗРАЧЕЊА

S. Doostmohammadi and S. J. Fatemi

Faculty of Physics, Shahid Bahonar University of Kerman, Kerman 76169-14111, Iran

E-mail: *doostmohammadi@sci.uk.ac.ir*

УДК 524.1-48-36

Оригинални научни рад

Електронске и мионске компоненте широких атмосферских лавина (ШАЛ) са енергијама већим од 10^{19} eV су анализирани на основу података са различитих великих детектора лавина. Особине лавина су проучаване за енергије мање и веће од $(3 - 4) \times 10^{19}$ eV. Параметар старости лавине, зенитни угао, зависност величине лавине од величине мионске компоненте као и од енергије при-

марне честице, указују на тежи масени састав примарног зрачења са енергијама већим од $(3 - 4) \times 10^{19}$ eV. Поређење експерименталних података о ШАЛ са резултатима симулација даје највише 20% фотона у примарном зрачењу енергија већих од 4×10^{19} eV. Правци стизања лавина тих енергија показују повећање концентрације ка супергалактичкој равни.